Title	Pairing correlations in the two-layer attractive Hubbard model
Author(s)	Zujev, Aleksander; Scalettar, Richard T.; Batrouni, George G.; Sengupta, Pinaki
Citation	Zujev, A., Scalettar, R. T., Batrouni, G. G., & Sengupta, P. (2014). Pairing correlations in the two-layer attractive Hubbard model. New Journal of Physics, 16(1), 013004-.
Date	2014
URL	http://hdl.handle.net/10220/18879
Rights	

Pairing correlations in the two-layer attractive Hubbard model

2014 New J. Phys. 16 013004

(http://iopscience.iop.org/1367-2630/16/1/013004)

New Journal of Physics
The open access journal at the forefront of physics
Deutsche Physikalische Gesellschaft DPG | IOP Institute of Physics

Pairing correlations in the two-layer attractive Hubbard model

Aleksander Zujev[1], Richard T Scalettar[2], George G Batrouni[3,4,5] and Pinaki Sengupta[1,6]

[1] School of Physical and Mathematical Sciences, Nanyang Technological University, 21 Nanyang Link, Singapore 637371, Singapore
[2] Department of Physics, University of California, Davis, CA 95616-8677, USA
[3] Institut Non-Linéaire de Nice, UMR 6618 CNRS, Université de Nice–Sophia Antipolis, 1361 route des Lucioles, F-06560 Valbonne, France
[4] Institut Universitaire de France, Maison des Universités, 103 Boulevard Saint-Michel, F-75005 Paris, France
[5] Centre for Quantum Technologies, National University of Singapore; 2 Science Drive 3, Singapore 117542, Singapore
E-mail: psengupta@ntu.edu.sg

Received 16 August 2013, revised 27 November 2013
Accepted for publication 2 December 2013
Published 2 January 2014
New Journal of Physics **16** (2014) 013004
doi:10.1088/1367-2630/16/1/013004

Abstract

Studies of systems with two fermionic bands (or equivalently, layers) with *repulsive* interaction strength U have a long history, with the periodic Anderson model (PAM) being one of the most frequently considered Hamiltonians. In this paper, we use quantum Monte Carlo to study analogous issues for *attractive* interactions. As in the PAM, we focus on a case where one band (layer) is uncorrelated ($U = 0$), and the effect of hybridization V between the bands (layers) on the pairing correlations. A key difference with the PAM is that there is no sign problem, so that we are better able to explore the physics of *doped* bilayer attractive systems at low temperatures (except in the case of exponentially small transition temperatures) whereas ground state properties of repulsive models can be determined only at half-filling. For small V, pairing in the $U < 0$ layer induces pairing in the $U = 0$ layer. At larger V superfluidity

[6] Author to whom any correspondence should be addressed.

is suppressed at the low but finite T at which the quantum Monte Carlo was performed. The quantum Monte Carlo data are complemented by results obtained with the Bogoliubov–de Gennes approximation.

1. Introduction

Cuprate superconductors are characterized by CuO_2 planes which are rather isolated from each other by intervening rare earth atoms. The larger ('c-axis') separation of Cu atoms perpendicular to the planes compared to the in-plane lattice constants (a, b) has focused theoretical attention on the magnetic and superconducting (SC) properties of two-dimensional (2D) models, most notably the square lattice Heisenberg and Hubbard Hamiltonians. Indeed, one of the most fundamental theoretical questions which arose in the initial investigations of possible models of high temperature superconductivity concerned the nature of the magnetism in the ground states of these Hamiltonians: were they spin-liquids or did they exhibit long range order (LRO)? It was established numerically [1–3] that both the Heisenberg Hamiltonian and the half-filled Hubbard Hamiltonian have long range antiferromagnetic (AF) order at $T = 0$. A still-unresolved question is the nature of pairing in the doped Hubbard Hamiltonian.

A natural extension of these single layer questions concerns the behavior of spin and pairing correlations in coupled layers. Interlayer connections are required to elevate the magnetic ordering, which is possible only at $T = 0$ in two dimensions, to the finite temperature Néel transitions observed experimentally. Similarly, the SC transition temperature tends to increase with the number of adjacent CuO_2 layers between the charge reservoirs, getting steadily larger from single layered $La_{2-x}Sr_xCuO_4$, to bilayer $YBaCu_3O_{6+y}$ to the HgBaCaCuO sequence where T_c peaks at about 130 K for materials with $n = 3$ layers [4]. Antiferromagnetism and thus superconductivity exhibit the expected behavior that having additional (non-frustrating) couplings, and increasing the dimensionality, enhances the tendency to order.

The route from 2D to three-dimensional (3D) is, however, not completely straightforward. Quantum Monte Carlo (QMC) studies of coupled Heisenberg layers [5], have shown that when the interlayer coupling grows sufficiently large, there is a quantum phase transition (QPT) from a ground state with long range magnetic order to a spin-gapped ground state, in which singlets form between pairs of spins in the two layers [6][7]. A similar effect is seen in QMC studies of the two-layer half-filled Hubbard Hamiltonian [7].

The basic phenomenon of singlet formation usurping magnetic order in itinerant fermion Hamiltonians does not crucially depend on having the same interaction strength U, or hopping t, for the two species. Indeed, a Hamiltonian with $U = 0$ in one (conduction) band and hopping $t = 0$ in another (localized) band, is the commonly encountered periodic Anderson model (PAM). At half-filling, for weak hybridization between the conduction and localized bands, AF order is present. As the hybridization grows bigger, however, 'Kondo-like' singlets form and destroy AF order. Thus the PAM exhibits a similar QPT as for two identical Hubbard layers ($t_1 = t_2$ and $U_1 = U_2$). This close similarity of the PAM and Hubbard bilayers emphasizes

[7] This AF-singlet transition in coupled layers is closely analogous to the difference between the magnetic correlations of odd and even rung ladders. An odd number of coupled one-dimensional chains is gapless and has power law decay of spin correlations, while even number of chains are gapped and have exponential decay. See [6].

that the physics of fermions in multiple layers can equivalently be interpreted in terms of multiple orbitals.

The purpose of this paper is to study the possibility of analogous phenomena in the case when there is an *attractive* interaction. More specifically, we examine the nature of pairing correlations for coupled planes (orbitals) in situations when an attraction is present only in one plane (orbital). We use the $U < 0$ Hubbard Hamiltonian as an appropriate simple model, and employ a combination of QMC and Bogoliubov–de Gennes (BdG) mean field theory. We will focus on a case analogous to that of the PAM, namely when $U = 0$ in one of the layers. We are interested in both how the interlayer hopping affects the s-wave pairing correlations in a layer with $U < 0$, and also whether pairing can be induced by a 'proximity effect' in the $U = 0$ layer. Such behavior would be directly analogous to the 'Ruderman–Kittel–Kasuya–Yoshida (RKKY)' spin polarization cloud which is induced in the conduction band by the presence of the local moments in the PAM. A particularly interesting issue is whether the QPT which occurs at commensurate filling is present also in the doped case.

Bilayer Hubbard Hamiltonians with attractive interactions which differ in the two layers have also been studied by Berg *et al* [8] and Wachtel *et al* [9]. The motivation is to explore the possibility of enhanced superconductivity, with transition temperatures approaching the mean field pairing scale Δ_0, by separating a spatial region where there is strong pairing but low phase stiffness, from a metallic region. The emphasis of this earlier work was on the case when the bandwidth W is much larger than Δ_0, whereas the focus here will be on an 'intermediate coupling' regime where $W \sim \Delta_0$. Our numerical work complements these previous methods, since we cannot easily access that part of parameter space which is in the Bardeen–Cooper–Schrieffer (BCS) limit and hence has exponentially small transition temperatures, regions which are however accessible to analytic studies. Experimental studies of superconductivity in systems in which one layer ($BaBiO_3$) provides the electron pairing interaction and the other layer ($BaPbO_3$) is conducting, which test some of the ideas of [8, 9] have also been reported. Indeed, the role of inhomogeneity, arising either spontaneously or introduced explicitly into the Hamiltonian, has been studied in a variety of contexts within the repulsive Hubbard model as well [10, 11].

The remainder of this paper is organized as follows: in section 2 we write down the precise model and give an overview of the QMC and BdG computational methodologies. Sections 3 and 4 present the BdG and QMC results, respectively. Section 5 recaps our conclusions.

2. Model and computational methods

Our starting point is the two layer (orbital) attractive Hubbard Hamiltonian

$$H = -t \sum_{\langle ij\rangle l\sigma} (c^\dagger_{il\sigma} c_{jl\sigma} + c^\dagger_{jl\sigma} c_{il\sigma}) - V \sum_{i\sigma} (c^\dagger_{i1\sigma} c_{i2\sigma} + c^\dagger_{i2\sigma} c_{i1\sigma}) - \sum_{il\sigma} \mu_l c^\dagger_{il\sigma} c_{il\sigma}$$
$$- \sum_i |U_1| \left(n_{i1\uparrow} - \frac{1}{2}\right)\left(n_{i1\downarrow} - \frac{1}{2}\right). \quad (1)$$

Here an intralayer kinetic energy term $c^\dagger_{il\sigma} c_{jl\sigma}$ describes the destruction of a fermion with spin σ on site j of layer l and its creation on site i of the same layer. A second interlayer kinetic energy term $c^\dagger_{il\sigma} c_{il'\sigma}$ hybridizes the two layers l, l'. Fermions of different spin feel an attractive

interaction $-|U_l|$ on layer l. The chemical potentials μ_l control the filling. Our lattice geometry consists of two coupled square lattice of linear size L. We choose $U_1 < 0$ in the 'SC' layer and $U_2 = 0$ in the metallic one.

At half-filling, a particle–hole transformation formalizes the similarity of the repulsive and attractive models. The vanishing of AF order with increasing V for $U > 0$ bilayers immediately implies that ground state pairing (and charge density wave order, with which it is degenerate) must be destroyed as V grows for $U < 0$. However, whereas AF order occurs only at half-filling (and only at $T = 0$) in the 2D repulsive Hubbard Hamiltonian, superconductivity appears away from half-filling, and at a finite (Kosterlitz–Thouless) transition temperature [30, 31], in the attractive Hubbard Hamiltonian. This opens up fundamentally new issues in the attractive case. The manner is which fermions on sites in adjacent layers lock into local objects and the interplay with LRO when the filling is incommensurate is an interesting question. The absence of a sign problem in the case of the attractive Hubbard model enables the study of low temperatures even when the filling is incommensurate, allowing access to ground state properties.

We perform 'determinant' QMC [14] simulations of the Hamiltonian, equation (1), by writing a path integral for the partition function Z. The exponential of the interaction term U_l is decoupled with a Hubbard–Stratonovich field which allows the trace of the remaining exponentials of quadratic forms of the fermion operators to be performed analytically. The result is a sum over configurations of the Hubbard–Stratonovich field with a weight which takes the form of the product of the determinants of two matrices of dimension the spatial lattice size, one for each spin species. In the case of attractive interaction the two matrices, and hence their determinants, are identical, so that the weight is a perfect square and there is no sign problem. In our simulations we have used a discretization $\beta = L\Delta\tau$ of the inverse temperature β with $\Delta\tau = 0.125$, and an exact exponentiation of the kinetic energy operator. These choices ensure that the systematic 'Trotter' errors are smaller than the statistical error bars for the pair structure factor. Most of our runs represent the averaged results of 40 independent simulations of 1000 measurement sweeps, specifically ten runs for each type of boundary condition (periodic/antiperiodic) in the x and y directions. This boundary condition averaging can be thought of as sampling additional discrete momenta values intermediate to those with just periodic boundary conditions, and is known to reduce finite size effects somewhat.

We present results here for the real space pair correlation functions in the two orbitals

$$\begin{aligned} P_l(j) &= \langle \Delta_{i+j,l} \Delta^\dagger_{i,l} \rangle, \\ \Delta^\dagger_{il} &= c^\dagger_{il\uparrow} c^\dagger_{il\downarrow} \end{aligned} \tag{2}$$

and also their associated structure factors

$$\mathcal{P}^l_{\mathrm{s}} = \frac{1}{N} \sum_j P_l(j) \tag{3}$$

as functions of interband hybridization V, on-site attraction U_l, density n and temperature T. The long distance behavior of $P_l(j)$ yields the square of the SC order parameter, as does the extrapolation of the structure factor to the thermodynamic limit.

Other quantities of interest are the average near-neighbor intra- and inter-layer hopping

$$T_{ll} = \langle c^\dagger_{il\sigma} c_{i+\hat{\delta}\, l\sigma} \rangle, \quad T_{ll'} = \langle c^\dagger_{il\sigma} c_{il'\sigma} \rangle \tag{4}$$

and the near-neighbor intra- and inter-layer pairing correlations

$$P_{ll} = \langle \Delta_{i+\hat{\delta},l} \Delta^{\dagger}_{i+\hat{\delta},l} \rangle, \quad P_{ll'} = \langle \Delta_{i,l} \Delta^{\dagger}_{i,l'} \rangle, \tag{5}$$

where $\hat{\delta} \equiv (1,0)$ or $(0,1)$. In order to study the possibility of superfluidity mediated by interlayer pairs, we also define the pairing correlations

$$\mathcal{P}^{\perp}_{\mathrm{s}} = \frac{1}{N} \sum_{j} \langle \tilde{\Delta}_{i+j} \tilde{\Delta}^{\dagger}_{i} \rangle, \tag{6}$$

where

$$\tilde{\Delta}^{\dagger}_{i} = c^{\dagger}_{i1\uparrow} c^{\dagger}_{i2\downarrow} + c^{\dagger}_{i2\uparrow} c^{\dagger}_{i1\downarrow} \tag{7}$$

is the inter-layer pair creation operator [15].

Equation (1) can also be studied in mean field theory via the solution of the BdG equations. In this approach, the four fermion (interaction) term is decoupled in the Hamiltonian itself,

$$\mathcal{H}_{\mathrm{eff}} = -t \sum_{\langle ij \rangle l\sigma} (c^{\dagger}_{il\sigma} c_{jl\sigma} + c^{\dagger}_{jl\sigma} c_{il\sigma}) - V \sum_{i\sigma} (c^{\dagger}_{i1\sigma} c_{i2\sigma} + c^{\dagger}_{i2\sigma} c_{i1\sigma}) - \sum_{il\sigma} \tilde{\mu}_{il} c^{\dagger}_{il\sigma} c_{il\sigma}$$

$$- \sum_{i} |U_1| [\Delta_{i1} c^{\dagger}_{i1\uparrow} c^{\dagger}_{i1\downarrow} + \Delta^{*}_{i1} c_{i1\downarrow} c_{i1\uparrow}]. \tag{8}$$

Here the gap $\Delta_{il} = \langle c_{il\uparrow} c_{il\downarrow} \rangle$ and density $\langle n_{il\sigma} \rangle = \langle c^{\dagger}_{il\sigma} c_{il\sigma} \rangle$ are determined self-consistently by diagonalizing the quadratic BdG Hamiltonian and putting together the eigenvalues and eigenvectors appropriately to compute refined values which are inserted back in the Hamiltonian in an iterative process. A related BdG treatment of superconductivity in the presence of randomness (spatially varying μ_i) is given in [16, 17]. $\tilde{\mu}_{il} = \mu + |U_l| \langle n_{il} \rangle / 2$ includes a site-dependent Hartree shift with $\langle n_{il} \rangle = \sum_{\sigma} \langle n_{il\sigma} \rangle$.

In the general case, when inhomogeneous terms are present in the Hamiltonian, or are expected to develop spontaneously, (like the charge and spin stripes of the doped, repulsive Hubbard model), the order parameter and densities are allowed to depend on site index and the diagonalization must be done numerically. If translation invariance is present, equation (8) can be diagonalized analytically by going to momentum space. The resulting momentum sums are typically still done numerically, but larger lattices can be studied. We have implemented both approaches in the work presented here.

Although inhomogeneous Hartree–Fock theory allows for spatial variation of the densities and SC order parameters, the expectation values in equation (8) are independent of imaginary time, unlike the fluctuating Hubbard–Stratonovich field in the QMC approach. This leads to a less accurate treatment of interparticle correlations, but a numerically much more simple problem. In particular, larger spatial lattices can be studied, and the BdG solution can exhibit broken symmetry so that Δ_l itself can be non-zero, rather than having to be extracted from the asymptotes of the correlation function equation (2). Hence the combination of QMC and BdG serves to provide complementary information.

We present only a brief set of results of BdG calculations, focusing on the values of the order parameter Δ_l as a function of the same parameters as varied in the QMC. As mentioned above, the asymptotic value of $P^{l}_{\mathrm{s}}(j)$ is a measure of Δ^2_l. The BdG approach, since it neglects

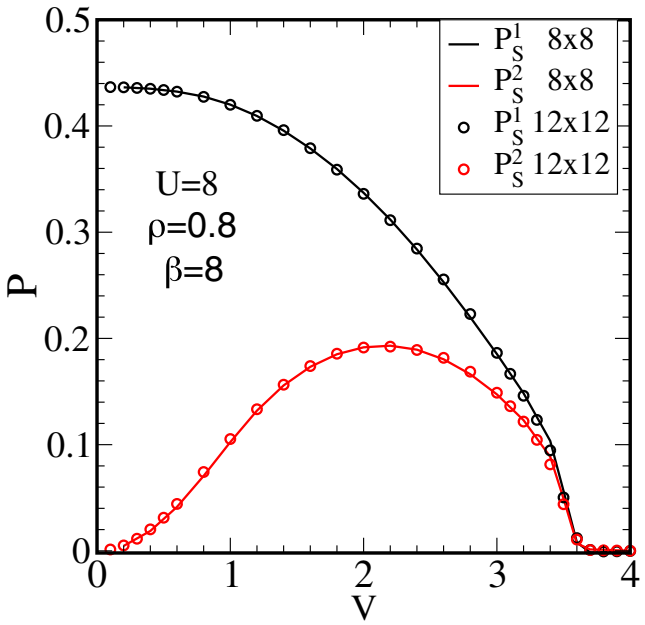

Figure 1. BdG result for 8×8 and 12×12 bilayer lattices, $\beta t = 8$, $U_1 = -8$ and $n = 0.8$. The figure shows that there is an induced SC in the non-interacting layer, with negligible finite size effects.

fluctuations, yields larger values of Δ_l than those of the QMC, which is an exact method. The main conclusion, is that, despite this difference in size of the order parameter, the qualitative physics— a dome-like induced pairing in the non-interacting layer— is similar in BdG and QMC.

3. Bogoliubov–de Gennes results

The results of BdG calculations are summarized in figure 1. We consider two layers with $U_1/t = -8$ and $U_2 = 0$, at a density of $n = 0.8$ electrons per site and study the evolution of the pairing correlation, Δ_l, in the two layers as a function interlayer coupling, V. Pairing in the correlated layer is suppressed by coupling to the non-correlated layer and eventually destroyed completely at $V \sim 3.6\,t$ for $\beta\,t = 8$. Whereas for $U_1 > 0$ there is a genuine quantum critical point so that the AF is destroyed above V_c even at $T = 0$, the destruction of superconductivity occurs here in the attractive case only because T is finite so that, as V increases, eventually the SC transition temperature T_c falls below $T = t/8$. Finite size effects are small at this temperature, so that a 12×12 lattice already captures the thermodynamic limit. For lower T, especially in regimes where the SC transition temperature is expected to be exponentially small, it is necessary to study larger lattices where discrete level spacings do not affect the results.

A further interesting feature of figure 1 is that the $l = 2$ layer, with $U_2 = 0$, develops induced pairing with the onset of interlayer coupling. The pairing amplitude, P_2, increases with increasing V up to a maximum before decreasing and eventually vanishing. Crucially, the pairing order parameter in *both layers* remains non-zero over a finite range of interlayer coupling—the induced pairing reported previously at half-filling extends to finite dopings. In the next section, we present extensive QMC results to confirm and complement these basic BdG results.

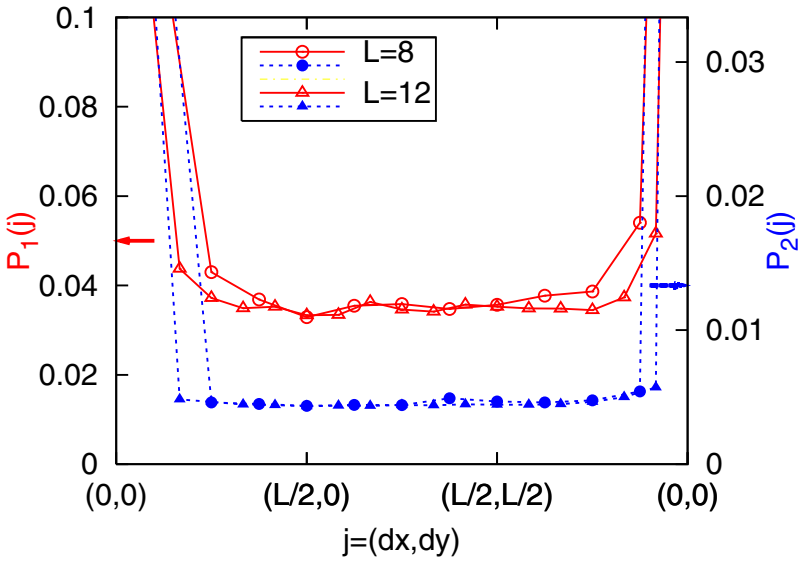

Figure 2. The dependence of the correlation functions, $P_{1,2}(j)$, on separation j in a bilayer system comprised of one correlated layer coupled to an uncorrelated layer for two different lattice sizes L. The system is at half-filling, $n = 1$, with interlayer hybridization $V = 0.8t$, and on-site interaction strength $U_1 = -6\,t$ for the correlated layer. The inverse temperature is $\beta\, t = 12$ and is sufficiently low that the ground state has been reached. The correlation functions converge to non-zero value at large separations, providing clear evidence for LRO. Despite the absence of interactions, there is proximity-effect induced LRO in the uncorrelated layer, $l = 2$, with an order parameter Δ_2 approximately a factor of three lower than for the correlated layer. As in figure 1, finite size effects are modest.

4. Quantum Monte Carlo results

4.1. Half filling

We begin our discussion of QMC results at half-filling, $n_1 = n_2 = 1$. As discussed, this corresponds to the particle–hole symmetric point $\mu_1 = \mu_2 = 0$ where there exists an exact mapping to the repulsive Hubbard model and the results can be benchmarked against previous studies for $U > 0$ [7, 12]. Lattices of the form $2 \times L \times L$, with $4 \leqslant L \leqslant 14$ were simulated with periodic boundary conditions over a wide range of interlayer hybridization, and on-site interaction for the interacting layer. An inverse temperature $\beta t = 12$ was used. In many of the cases we studied this was found to be sufficient for the observables to have converged to their ground state values. However, in some parameter regimes, the transition temperatures assume a BCS form and vanish exponentially, so that the pairing order is not easily accessible.

The spatial dependence of the pair correlations $P_l(j)$ at half-filling ($n = 1$), interlayer hybridization $V = 0.75t$, and interactions $U_1 = -6\,t$, $U_2 = 0\,t$ is shown in figure 2. The separation j follows a trajectory along the x-axis to maximal x separation $(\frac{L}{2}, 0)$ on a lattice with periodic boundary conditions, and then to $(\frac{L}{2}, \frac{L}{2})$ before returning to separation $(0, 0)$. Results for lattices with $L = 8, 12$ are shown in the figure. The interacting layer $l = 1$ exhibits clear LRO with $P_1(j)$ nearly independent of j beyond a separation of approximately $\frac{L}{4}$. The non-interacting layer $l = 2$ also exhibits proximity-effect induced LRO, although the correlation function is roughly three times smaller. This corresponds to an order parameter $\Delta_2 \sim \Delta_1/3$.

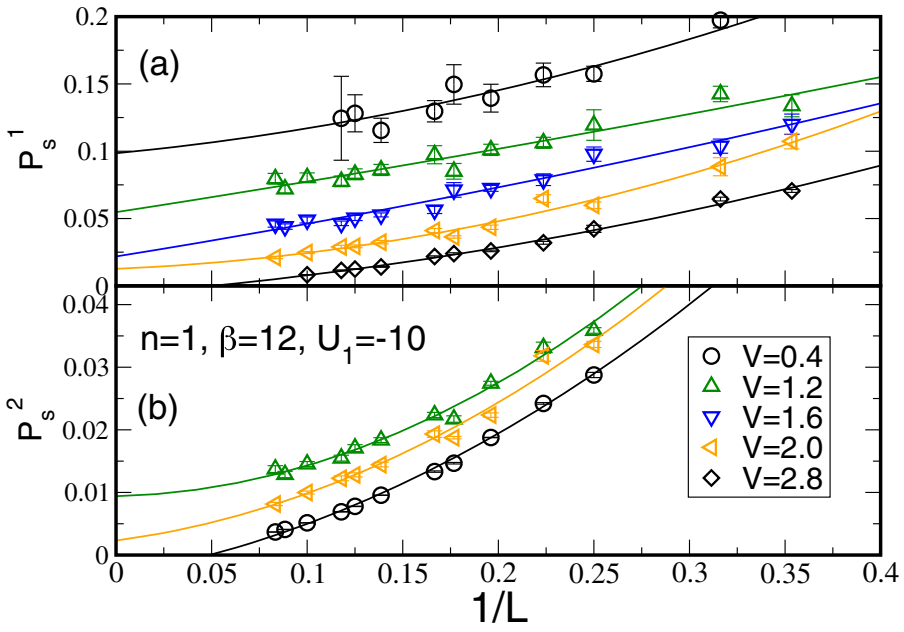

Figure 3. Finite size scaling analysis of the pair structure factor for a bilayer at half-filling and attractive on-site interaction in the correlated layer $U = -10\,t$: P_s^l are shown for different interlayer hoppings V as a function of inverse linear lattice size $1/L$. Top panel: the pair structure factor in the correlated layer, P_s^1. For interlayer hybridization $V \lesssim 2.0$ the extrapolated structure factor is non-zero indicating the existence of LRO. Bottom panel: the pairing structure factor P_s^2 in the non-interacting layer. For intermediate V, P_s^2 is non-zero, signaling the presence of induced pairing. For small V, data are shown only for systems with linear size up to $L = \sqrt{72}$. See text.

Figures 3 and 4 show an analysis of the pair structure factor, equation (3), which sums the real space correlations of figure 2. Figure 3 provides a finite size scaling analysis for data on different lattice sizes at several values of the interlayer hybridization V. Data are obtained both for 'standard' ($L \times L = 6 \times 6,\ 8 \times 8, \ldots$) tilings and also for square lattices which are rotated relative to the primitive axes (e.g. $4\sqrt{2} \times 4\sqrt{2}$, $6\sqrt{2} \times 6\sqrt{2}$, etc). Data are fit to a linear plus quadratic form

$$P_s^l(L) = P_s^l(\infty) + A/L + B/L^2, \tag{9}$$

where the linear in $1/L$ term is the expected spin-wave correction to the thermodynamic limit value $P_s^l(\infty)$ in the ordered phase [32], and the quadratic in $1/L^2$ term describes the $1/N$ fall-off of the structure factor which occurs when the real-space correlations are short-ranged (see equation (3)). We found the structure factor data to fluctuate more strongly at small V, precluding the acquisition of data for linear dimension $L > \sqrt{72}$. For larger V, lattices of up to $L = 12$ were studied.

The extrapolated results are then given in figure 4. Increasing the interlayer hybridization reveals that the pair structure factor for the interacting layer, P_s^1, decreases monotonically and eventually the intra-layer pairing is destroyed at some critical V_c. On the other hand, the pairing structure factor for the non-interacting layer P_s^2 varies non-monotonically with V. It vanishes (or is exponentially small at low but finite T) as $V \to 0$. As V increases, long-range pairing

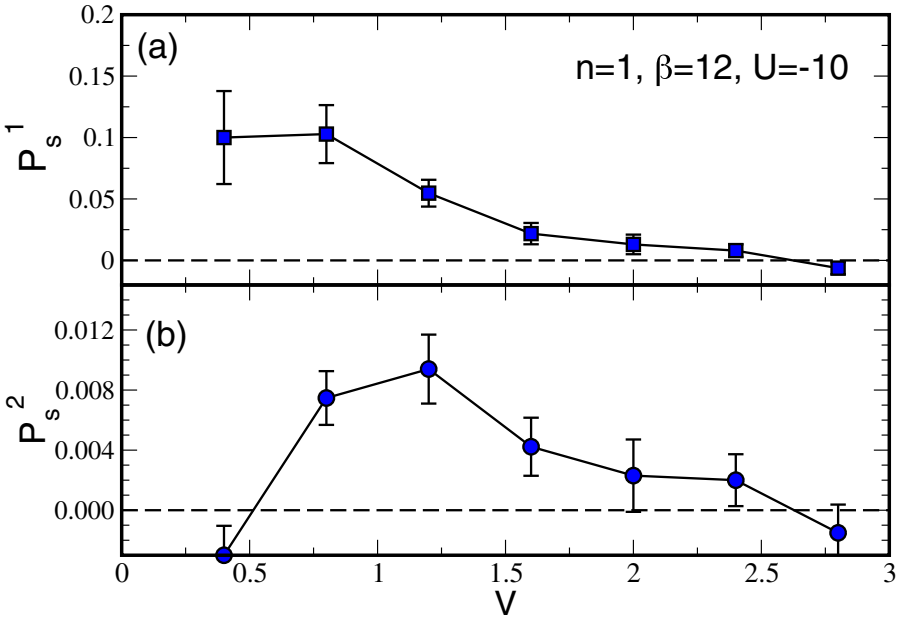

Figure 4. Extrapolated values (from figure 3) of the pair structure factor for a bilayer at half-filling and attractive on-site interaction in the correlated layer $U = -10\,t$, as a function of the interlayer coupling, V. Top panel: the pair structure factor in the correlated layer, P_s^1. Bottom panel: the pairing structure factor P_s^2 in the non-interacting layer. P_s^2 increases from zero for $V > 0$, signaling the onset of induced pairing. With further increase of V, LRO vanishes simultaneously in both layers.

correlations become more robust, reach a maximum at an intermediate V (which, as we shall later show, depends on the strength of on-site interaction in the interacting layer) and then decrease continuously to zero at V_c. For $V > V_c$, the ground state is dominated by *inter*-layer singlets. Obtaining a precise value of V_c is complicated by the error bars in the raw data for each lattice size and then additional uncertainties in the extrapolation of figure 3. Our data suggest that P_s^2 and P_s^1 are zero to within error bars for $V \gtrsim 2.0$ and have certainly vanished for $V > 2.5$.

4.2. Incommensurate filling

We now turn to the case of doped layers. As mentioned in the introduction, this is interesting for two reasons. Firstly, there is a possibility of a finite temperature Kosterlitz–Thouless transition because the charge density wave (CDW)-SC symmetry is broken. Secondly, simulations of coupled, doped repulsive layers at low T are not possible. Hence there is no determinant QMC (DQMC) information available for the nature of magnetism in coupled layers away from half-filling. Our simulations address this issue, albeit for attractive on-site interactions.

The results in figures 5 and 6 confirm that induced pairing in the uncorrelated layer extends to finite dopings away from half-filling; indeed the pair correlation functions in the two layers are qualitatively similar to those at half-filling. Pairing in the correlated layer decreases monotonically to zero at a finite V_c. In the non-interacting layer, pairing increases rapidly from zero as the interlayer hybridization is turned on, reaches a maximum value at intermediate V and then decreases to zero. We expect however, that unlike the half-filled case where the vanishing

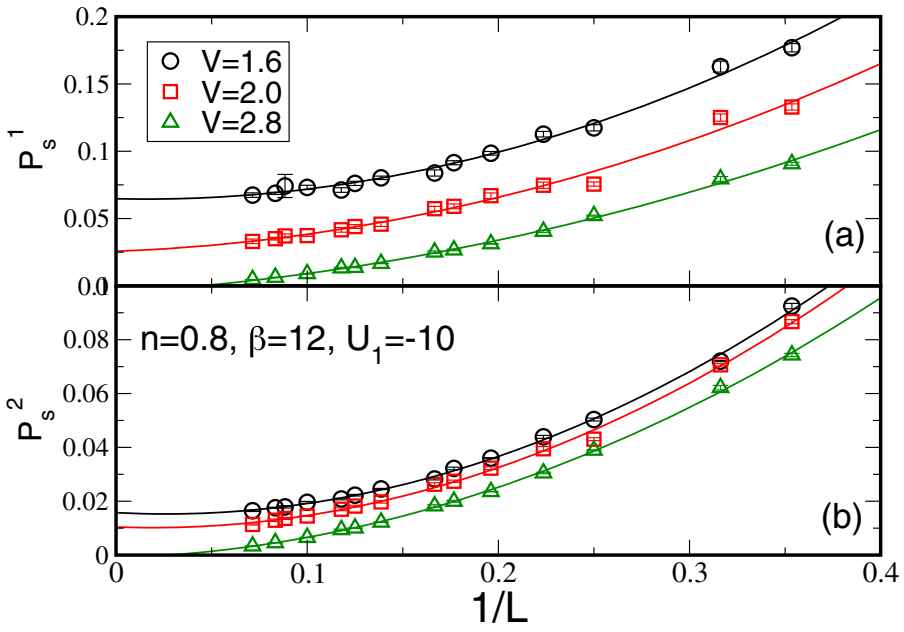

Figure 5. Finite size scaling for the pair structure factor for a bilayer away from half-filling, $n = 0.8$, for attractive on-site interaction in the correlated layer $U_1 = -10\,t$. As at half-filling, the extrapolation to zero vanishes for large enough interlayer hybridization V.

of pairing at large V occurs even at $T = 0$ (reflecting a QPT), in the doped case it is most likely that pair correlations become short ranged because the transition temperature falls below the simulation temperature as V increases. Because the transition temperature is suppressed exponentially in the BCS regime, it is not possible to perform the simulations at the extremely low T needed to settle this issue.

At intermediate to strong values of the on-site interaction ($|U| \gtrsim 6\,t$), the ground state of a system of coupled correlated and uncorrelated layers away from half-filling consists of intra-layer pair formation in *both* layers over a finite non-zero range of interlayer coupling. Eventually, at sufficiently strong interlayer hybridization, the system is characterized by singlet formation between the layers, and pairing occurs only at a (much) reduced temperature. We find here that induced pairing is found to be absent for $|U| \lesssim 6t$ at an inverse temperature $\beta t = 12$. The simulation results are summarized in figure 6 where the extrapolated pairing structure factors for the two layers are shown as a function of the interlayer hybridization V for some representative values of the on-site interaction in the correlated layer, and at a fixed value of the density, $n = 0.8$. The maximum of the pairing structure factor in the uncorrelated layer and the critical value of interlayer coupling for suppression of pairing increases with $|U|$. Our results are consistent with the disappearance of pairing in both layers occurring simultaneously in these finite T simulations. The error associated with determining the extrapolated pairing structure factor in the thermodynamic limit constrains the accuracy with which V_c can be determined to about $\pm 0.2t$. In a marked departure from the BdG results, the QMC data show that a finite non-zero interlayer coupling is required for the onset of induced pairing in the uncorrelated layer at $\beta t = 12$.

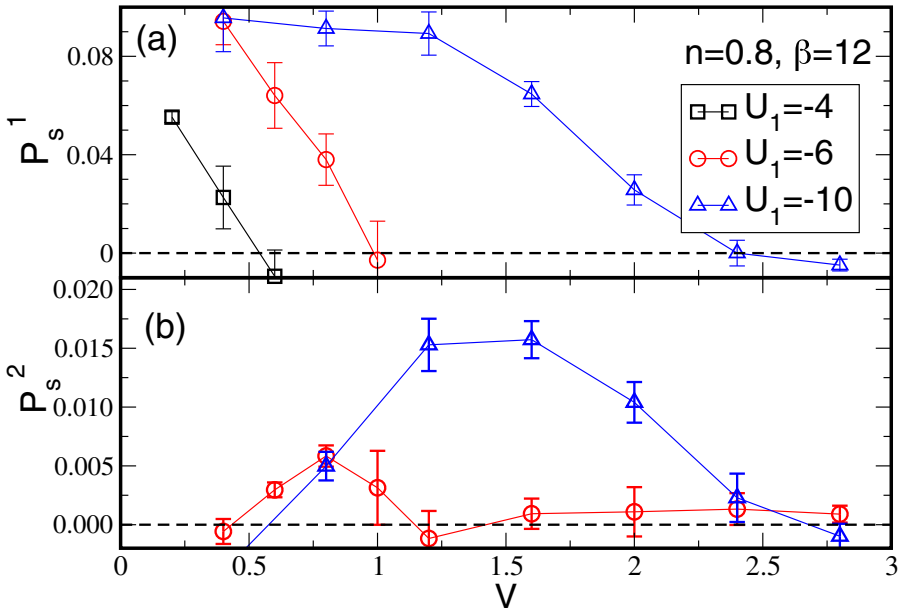

Figure 6. Extrapolated value (thermodynamic limit $L \to \infty$) for the pair structure factor for a bilayer away from half-filling, $n = 0.8$, for three representative values of the attractive on-site interaction in the correlated layer: $U_1 = -4\,t, -6\,t, -10\,t$. For $|U_1| \lesssim 6\,t$, $P_s^2 = 0$ at all values of V, indicating the absence of induced pairing, or else pairing only at very low T below those simulated. At stronger on-site interaction ($|U_1| \gtrsim 6\,t$) in the correlated layer, induced pairing appears in the uncorrelated layer over a finite range of V. The critical V_c for suppression of intra-layer pairing increases with $|U_1|$.

Figure 6 shows that P_s^1 increases systematically for $V > 0.5$ as U changes from $U = -4$ to -10. In the case of the repulsive Hubbard Hamiltonian at half-filling the magnetic response first increases with U but then reaches a maximum at $U \sim 8t$ before falling. This behavior is understood qualitatively from the fact that the superexchange $J = 4\,t^2/U$ which provides the large U magnetic energy scale declines with U. Thus, for example the Néel temperature of the 3D Hubbard model at half-filling is maximized at $U \sim 8t$. The analogue in the attractive Hubbard model is that the pairs become heavy, with an effective hopping $t_{\rm eff} \sim t^2/U$ as a consequence of the (temporary) pair-breaking that must occur as a pair hops. This analogy suggests the pairing response might also be maximal at an intermediate U. Because of the sign problem, it is not known from DQMC whether such a non-monotonic behavior exists in the repulsive model away from half-filling, or, if it does, at what value of U the maximum occurs. In any case, the issue of an optimal U is a bit subtle. At a fixed non-zero temperature, the t^2/U energy scale can fall below T, leading to a decrease in order at strong coupling. However, strictly at $T = 0$ the AF order parameter in the repulsive Hubbard model, for example, increases monotonically to the large U Heisenberg value [13].

In some cases the data are more well behaved (smaller error bars) at $\rho = 0.8$ (figures 5 and 6) than at $\rho = 1.0$ (figures 3 and 4). We believe this is a consequence of the degeneracy between charge density wave and SC order at half-filling. There is a tendency, for $\rho = 1$ and especially at low T, for the system to get stuck in one of the competing ordered phases, leading to larger fluctuations between runs. This degeneracy is lifted away from half-filling.

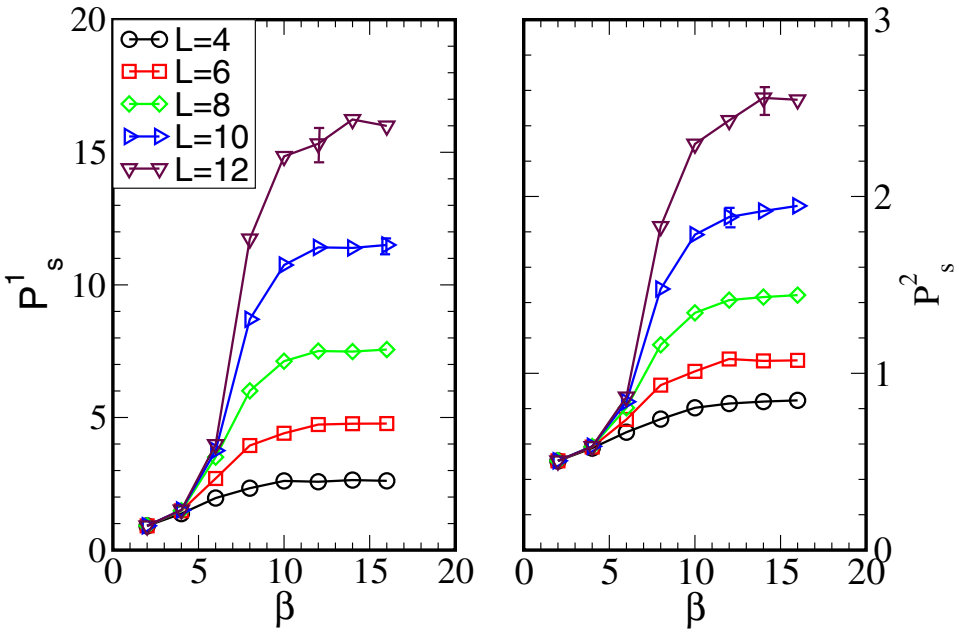

Figure 7. Dependence of pair structure factors P_s^l on inverse temperature β showing that ground state has been reached at $\beta t = 12$ for this parameter set, $n = 0.8$, $U = -10$, $V = 1.2$ and lattice sizes $N = 4$, 6, 8, 10 and 12. Note difference in scales between the structure factor on layer 1 (left), where $U_1 = -10$, and on layer 2 (right), where $U_2 = 0$ and superconductivity must be induced by the proximity effect. Representative error bars are shown.

Throughout these calculations an important question is whether the temperatures are low enough for the ground state, and its associated order, if any, to have been reached. Figure 7 provides one measure of this by showing the pair structure factors versus β for $n = 0.8$, $U = -10$ and $V = 1.2$. From such plots we conclude that $\beta\, t \approx 12$ is sufficiently cold. Hence this is the value of inverse temperature chosen throughout this paper. It is important to emphasize, however, that the required value of β will depend on filling, lattice size and the energy scales of the model. Small lattices generally reach their ground states at higher temperature, since it is easier for the correlation length to exceed the lattice size. More problematic than large lattices, however, are situations where an exponentially small BCS pairing temperature scale is possible. We expect this to occur for doped lattices at small V. Hence it is possible that some situations where the extrapolated structure factor vanishes arise from the pairing scale falling below the temperature at which the simulation is performed. An exponentially small scale is not possible to pursue numerically.

Having established the existence of induced pair formation at finite doping and the evolution of the associated structure factor with V, we investigate the dependence of the pairing phenomenon on the density of electrons in the layers. Our results (figure 8) show that induced pairing occurs generically at all densities and that the pairing structure factor behaves in a qualitatively similar manner. In the single layer (2D) attractive Hubbard Hamiltonian, T_c rises abruptly from zero at half-filling where charge density order competes with pairing, but then shows a gradual decline below an optimal doping [30]. Our data in figure 8 suggest the increase in pairing might be saturating in the range $\rho \sim 0.6$–0.8. If this two layer model were to behave like the single layer case, this saturation would be followed by a decline with further doping away from $\rho = 1$.

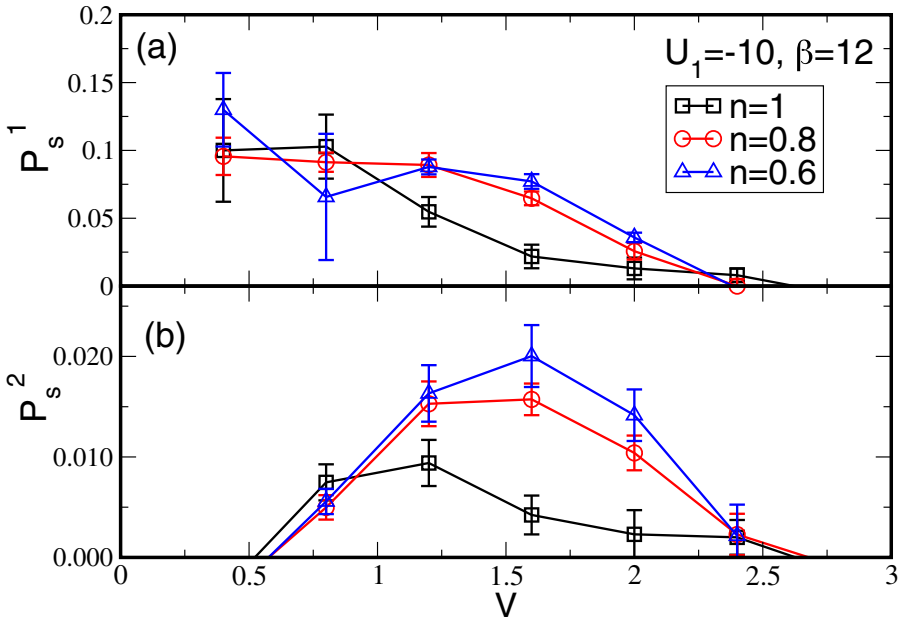

Figure 8. The pair structure factors at various filling values and $U_1 = -10$. Induced pairing occurs at all densities, with the amplitude of induced pairing increasing with doping away from half-filling. Insets: finite size scaling for $n = 0.8$. Inverse temperature $\beta t = 12$.

4.3. Nature of the phase at $V > V_c$

In section 4 we saw that when the interlayer hybridization, V, is larger than a threshold value V_c, the intra- and inter-layer pair structure factors are strongly suppressed at fixed, non-zero T. While the value of V_c depends on the filling and the interaction strength in the correlated layer, we found it to be typically $V_c \sim 2t$. The question then arises as to the nature of the correlations for $V > V_c$.

To address this question, we show in figure 9 the average intra- and inter-layer hopping, equation (4), and the short range (near neighbor) pair correlations, equation (5) for the half filled system. We see that as V increases, the interlayer near neighbor hopping, T_{12}, and pairing correlations, P_{12}, increase monotonically and saturate when $V > V_s$ with $V_s \approx 4t$. At the same time, the corresponding intra-layer quantities decrease and become negligible $V_s \approx 4t$. This value of V_s is quite insensitive to the value of U_1.

This behavior can be understood by recalling that in the limit of $U_1 = 0$, there is a sharp phase transition from a metal to a Mott insulator when a finite gap opens in the dispersion relation, $E^{\pm}(k_x, k_y) = \pm V - 2t(\cos k_x + \cos k_y)$ for $V = V_s = 4t$. One way of interpreting the results of figure 9 is that, as $|U_1|$ is increased from zero, a crossover line continues above this non-interacting critical point at $U_1 = 0$. Our results indicate that the trajectory of this crossover line is fairly vertical in the V-U_1 layer, i.e. V_s is only weakly U_1 dependent.

Our results indicate that, for half-filling, in the region above, but close to, $V_c \approx 2t$, long range pairing order vanishes, but short range intralayer correlations are still present. These decrease as V grows. When $V > V_s \approx 4t$, a crossover occurs in which short range intralayer correlations are completely suppressed- the particles in interlayer nearest neighbor sites form independent pairs.

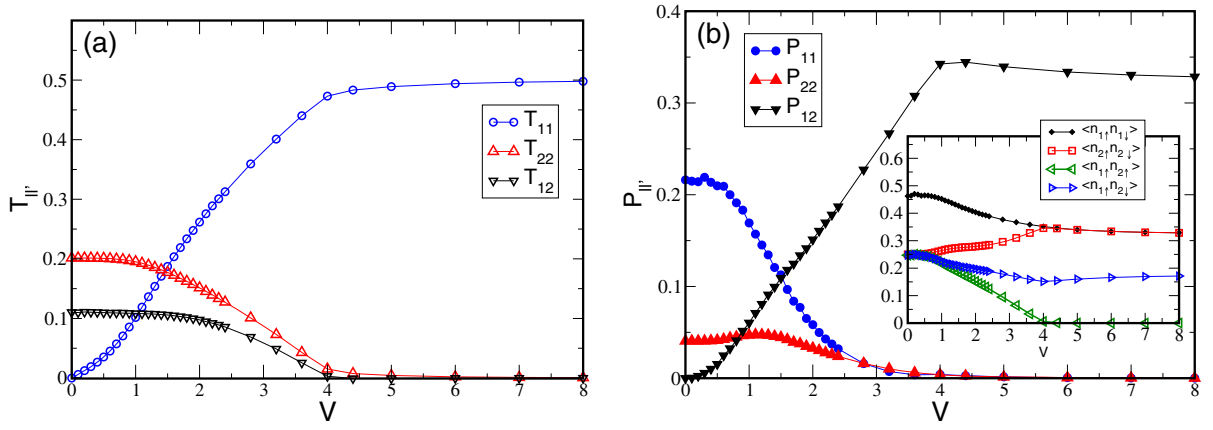

Figure 9. Short range correlations for the half filled system at $U_1 = -10$. Top: intra-layer (T_{11}, T_{22}) and interlayer (T_{12}) near neighbor hopping. The intra-layer hopping vanishes in both layers at $V \equiv V_s = \approx 4\,t$, while interlayer hopping increases and reaches maximum. Bottom: intra-layer (P_{11}, P_{22}) and interlayer (P_{12}) near neighbor pairing correlations. The intra-layer pairing vanishes in both layers at $V = V_s$, while interlayer hopping increases and reaches maximum. Inset: on-site density–density correlations, $\langle n_1(\mathrm{i},\uparrow)n_1(\mathrm{i},\downarrow)\rangle$, $\langle n_2(\mathrm{i},\uparrow)n_2(\mathrm{i},\downarrow)\rangle$ and near neighbor interlayer density–density correlations, $\langle n_1(\mathrm{i},\uparrow)n_2(\mathrm{i},\uparrow)\rangle$, $\langle n_1(\mathrm{i},\uparrow)n_2(\mathrm{i},\downarrow)_2\rangle$. The onset of interlayer pairing corresponds to the vanishing of interlayer nearest neighbor up–up density–density correlation at $V_s = 4\,t$. Error bars for these local quantities are of the order of, or smaller than, the symbol size.

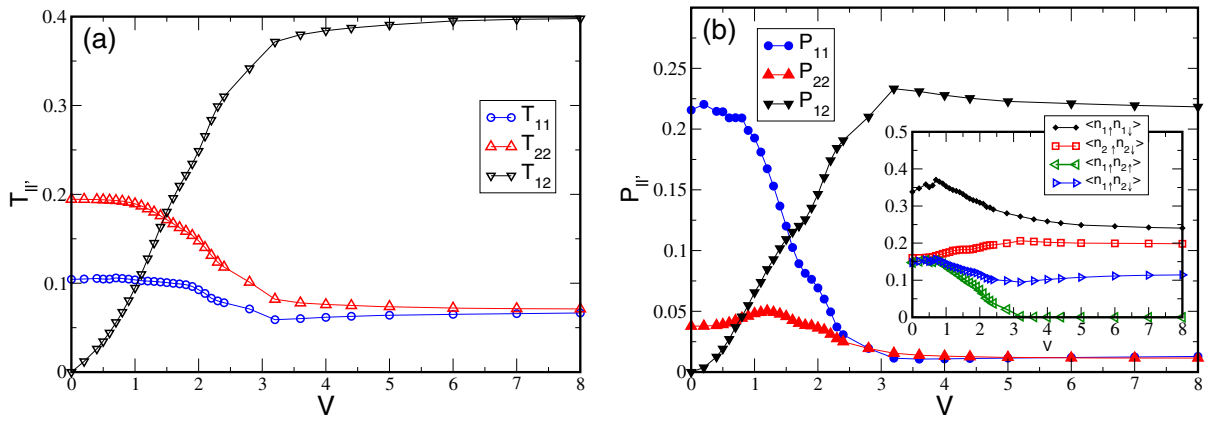

Figure 10. Short range correlations for the doped system at $n = 0.8$, $U_1 = -10$. Top: near neighbor hopping. The intra-layer hopping decreases and reaches non-zero limiting value in both layers at $V \approx 3t$, while the interlayer hopping increases and reaches maximum. Bottom: near neighbor pairing correlation. The intra-layer pairing vanishes in both layers at $V \approx 3t$, while interlayer hopping increases and reaches maximum. Inset: on-site and near neighbor interlayer density–density correlations. The onset of interlayer pairing corresponds to the vanishing of interlayer nearest neighbor up–up density–density correlation at $V \approx 3t$. Error bars for these local quantities are of the order of, or smaller than, the symbol size.

When the system is doped, it exhibits some similarities to the half-filled case. The results for $T_{ll'}$ and $P_{ll'}$ are shown in figure 10 for $n = 0.8$. Densities $n = 0.6$, 0.4, 0.25 and 0.2 (not shown), all display the same qualitative behavior. The main difference between half-filled and

doped lattices is that when T_{12} reached its saturation value for $V > V_s$, T_{11} and T_{22} do not vanish. The reason is that the interlayer pairs which form due to strong interlayer hybridization are still mobile, the band is not full due to the doping. To study the possibility that these mobile interlayer pairs might condense to a superfluid, we measured the interlayer pair correlations equation (6) for several fillings, n, and values of V. We find no evidence for such superfluid behavior. This is likely to be caused by the finite T at which the QMC is performed. If the pairs are in the BCS regime, the temperature at which SF will develop will be exponentially low.

5. Conclusions

In this paper we have used QMC to elucidate the properties of a multi-orbital *attractive* Hubbard Hamiltonian. Our key conclusions are the quantification of the induced pairing in a non-interacting orbital by superconductivity in a correlated orbital, and, conversely, the suppression of pairing in an orbital with an attractive interaction through its coupling to a non-interacting orbital, in the intermediate coupling regime $U_1 \sim W = 8t$. The general trends of the evolution of the order parameters are similar to those found in BeG mean field theory.

As we have emphasized in the introduction, analogous issues for repulsive models have a long history. In fact, over the last 4–5 years, the question of 'orbitally selective Mott transitions', has been extensively explored. The fundamental objective has been an examination of the density of states to determine whether or not one subsystem can be metallic (zero energy gap at E_F) and the other insulating (non-zero gap), or whether the coupling forces the transition to occur simultaneously in all orbitals (layers) [18–29]. Our work suggests that for attractive interactions the suppression of superconductivity at large inter-orbital hybridization V seems typically to occur simultaneously. It is to be noted, however, that it appears that at weak V pairing can exist in the correlated orbital before it is induced in the non-interacting one. That is, we find that for the attractive case at small interlayer coupling, SC exists only in the interacting layer despite the fact that at larger V the vanishing of SC appears at a common V_c.

This paper has focused on the evolution of the pair structure factor with the hybridization V between the attractive and non-interacting layers at low temperatures. At weak V there is no LRO in the $U = 0$ layer, however there is an onset of induced pairing at intermediate $V \sim 1.5t$ if U is sufficiently large. Further increase in V returns the layer to a phase in which long range pairing is suppressed. This non-monotonic behavior is qualitatively similar to the evolution of T_c reported in [8, 9], despite the rather different parameter regimes being studied there ($|U| \sim t$ and no hopping, or only one dimensional hopping, between the attractive U sites). This induced SC dome found in QMC is similar to that seen in the BdG treatment. The doping dependence of the critical temperature in a system with localized attractive orbitals coupled to a conduction band has also been explored [34].

Our work is related to several other recent determinant QMC and Lanczos studies of the attractive Hubbard model. Assman *et al* [33] found that in an attractive Hubbard model with a smoothly varying chemical potential (such as would be present in a confined ultracold atomic cloud) pairing is significantly increased in the half-filled portion of the lattice through its contact with doped regions. That is, the suppression of superconductivity caused by the appearance of a degenerate charge density wave phase at $n = 1$ is eliminated. Paiva *et al* [35] explored a one-dimensional model of borocarbides in which $U < 0$ and $U = 0$ sites alternate. Superconductivity is found to be possible only above a critical density.

We note that it was recently shown in repulsive models with more than two layers that there can be further non-trivial evolution of magnetic properties with the hopping across an interface between a Mott insulator and a metal [36]. It would be interesting to pursue related questions in the attractive model and, in particular whether the formation of a layer of local pairs at the boundary can lead to a shielding of penetration effects.

Finally, we investigated the nature of a state emerging at high interlayer hybridization V and find that it creates interlayer pairs, which at half-filling are stationary in the sense of a vanishing (or very small) intralayer kinetic energy T_{ll}. At incommensurate filling these pairs remain mobile at large V, with finite T_{ll}. We do not find evidence for the presence of any associated long-range pairing order, but that is most likely due to the finite T at which the QMC simulations are performed. One expects that for doped bands in two dimensions, pairing will cause superfluidity at $T = 0$.

Acknowledgments

We thank Simone Chiesa and Axel Euverte for very helpful discussions. We also thank Dror Orgad, Thomas Maier and Steven Kivelson for their helpful comments. This work was supported in part by a Tier 1 grant from the Ministry of Education (MOE), Singapore, by an ARO Award W911NF0710576 with funds from the DARPA OLE Program, by the CNRS-UC Davis EPOCAL LIA joint research grant; and by the CNRS-National University of Singapore FSQL LIA joint research grant. We also received laboratory collaboration funding from the University of California, Office of the President.

References

[1] Reger J D and Young A P 1988 *Phys. Rev.* B **37** 5978
[2] Hirsch J E and Tang S 1989 *Phys. Rev. Lett.* **62** 591
[3] White S R, Scalapino D J, Sugar R L, Loh E Y Jr, Gubernatis J E and Scalettar R T 1989 *Phys. Rev.* B **40** 506
[4] Shimizu S, Iwai S, Tabata S I, Mukuda H, Kitaoka Y, Shirage P M, Kito H and Iyo A 2011 *Phys. Rev.* B **83** 144523
Shimizu S, Tabata S I, Iwai S, Mukuda H, Kitaoka Y, Shirage P M, Kito H and Iyo A 2012 *Phys. Rev.* B **85** 024528 and references cited therein
[5] Sandvik A W and Scalapino D J 1994 *Phys. Rev. Lett.* **72** 2777
[6] For example, Dagotto E and Rice T M 1996 *Science* **271** 618
[7] Scalettar R T, Cannon J W, Scalapino D J and Sugar R L 1994 *Phys. Rev.* B **50** 13419
[8] Berg E, Orgad D and Kivelson S A 2008 *Phys. Rev.* B **78** 094509
[9] Wachtel G, Bar-Yaacov A and Orgad D 2012 *Phys. Rev.* B **86** 134531
[10] Emery V J, Kivelson S A and Lin H Q 1990 *Phys. Rev. Lett.* **64** 475
[11] Mondaini R, Ying T, Paiva T, Chiesa S and Scalettar R T 2012 *Phys. Rev.* B **86** 184506 and references cited therein
[12] Vekic M, Cannon J W, Scalapino D J, Scalettar R T and Sugar R L 1995 *Phys. Rev. Lett.* **74** 2367
[13] Varney C N, Lee C R, Bai Z J, Chiesa S, Jarrell M and Scalettar R T 2009 *Phys. Rev.* B **80** 075116
[14] Blankenbecler R, Scalapino D J and Sugar R L 1981 *Phys. Rev.* D **24** 2278
[15] Bulut N, Scalapino D J and Scalettar R T 1992 *Phys. Rev.* B **45** 5577
[16] Ghosal A, Randeria M and Trivedi N 1998 *Phys. Rev. Lett.* **81** 3940
[17] Ghosal A, Randeria M and Trivedi N 2001 *Phys. Rev.* B **65** 014501
[18] Liebsch A 2004 *Phys. Rev.* B **70** 165103

[19] Liebsch A 2005 *Phys. Rev. Lett.* **95** 116402
[20] Arita R and Held K 2005 *Phys. Rev.* B **72** 201102
[21] Inaba K and Koga A 2006 *Phys. Rev.* B **73** 155106
[22] Costi T A and Liebsch A 2007 *Phys. Rev. Lett.* **99** 236404
[23] Koga A, Kawakami N, Rice T M and Sigrist M 2004 *Phys. Rev. Lett.* **92** 216402
[24] Ferrero M, Becca F, Fabrizio M and Capone M 2005 *Phys. Rev.* B **72** 205126
[25] de'Medici L, Georges A and Biermann S 2005 *Phys. Rev.* B **72** 205124
[26] Rüegg A, Indergand M, Pilgram S and Sigrist M 2005 *Eur. Phys. J.* B **48** 55
[27] Inaba K, Koga A, Suga S I and Kawakami N 2005 *Phys. Rev.* B **72** 085112
[28] Knecht C, Blumer N and van Dongen P G J 2005 *Phys. Rev.* B **72** 081103
[29] Biermann S, de'Medici L and Georges A 2005 *Phys. Rev. Lett.* **95** 206401
[30] Scalettar R T, Loh E Y Jr, Gubernatis J E, Moreo A, White S R, Scalapino D J, Sugar R L and Dagotto E 1989 *Phys. Rev. Lett.* **62** 1407
[31] Moreo A and Scalapino D J 1991 *Phys. Rev. Lett.* **66** 946
[32] Huse D A 1988 *Phys. Rev.* B **37** 2380
[33] Assmann E, Chiesa S, Batrouni G G, Evertz H G and Scalettar R T 2012 *Phys. Rev.* B **85** 014509
[34] Koga A and Werner P 2011 *J. Phys.: Conf. Ser.* **302** 012040
[35] Paiva T, El Massalami M and dos Santos R R 2003 *J. Phys.: Condens. Matter* **15** 7917
[36] Euverte A, Hebert F, Chiesa S, Scalettar R T and Batrouni G G 2012 *Phys. Rev. Lett.* **108** 246401